Neurochemical Research (2026) 51:265
https://doi.org/10.1007/s11064-026-04884-7

RESEARCH

The Senescent Phenotype of Cultured Hypothalamic Astrocytes from Rats with Streptozotocin-Induced Dementia

Vanessa-Fernanda Da Silva[1,3] · Daniele Schauren da Costa[1] · Vitor Gayger-Dias[1] · Thomas Michel Sobottka[1] · Ana Carolina Ribeiro Da Silva[1] · Bruna Cristiana R. Biolchi[1] · Laíse Freese da Silva[1] · Nikoli Zasso[1] · Fernanda Becker Weber[1] · Izaviany Schimitz[1] · Diorlon Nunes Machado[1] · Carlos Alexandre Netto[1,2] · Marina Concli Leite[1] · Larissa Daniele Bobermin[1,2] · André Quincozes-Santos[1,2] · Carlos-Alberto Gonçalves[1,2]

Received: 1 July 2026 / Revised: 13 August 2026 / Accepted: 28 August 2026 / Published online: 11 September 2026
© The Author(s) 2026

Abstract

Alzheimer's disease (AD) is the most prevalent form of dementia, with aging as its primary risk factor. Among experimental models of sporadic AD, intracerebroventricular (ICV) administration of streptozotocin (STZ) in rodents is widely used. We hypothesized that STZ accelerates the process of cellular senescence, which in astrocytes can be assessed using classic markers, including p16, β-galactosidase, Lamin B1, and the senescence-associated secretory phenotype (SASP). To explore this, we cultured hypothalamic astrocytes from adult male Wistar rats at four weeks after STZ-ICV model induction to investigate whether the astroglial changes observed in vivo were maintained under in vitro conditions, and whether markers of senescence were more evident in astrocytes from STZ animals. As in the STZ dementia model, astrocyte cultures exhibited reduced levels of glutamine synthetase and glutathione. Furthermore, elevations in the transcription factors, FOXO3a, Nrf2, and NF-κB, were observed. Markers of unfolded protein response (CHOP and sorcin) were also increased in astrocytes from STZ animals. When evaluating senescence parameters, increases in p53, p21, and p16 were observed, while Lamin B1 levels remained unchanged. With regard to SASP, modulations in TNFα and extracellular HMGB1 and S100B levels also suggested the induction of a senescent profile. Taken together, these findings demonstrate that cultured astrocytes retain key alterations observed in the in vivo model of STZ-induced dementia, highlighting its usefulness for studying AD and therapeutic strategies. Observations in cultures suggest that STZ indeed induces astrocyte senescence and that S100B may be included as a component of the astroglial SASP.

Keywords Alzheimer's disease · Astrocyte · Neuroinflammation · SASP · Senescence · S100B

Introduction

Alzheimer's disease (AD) is the most frequently diagnosed dementia, and accounts for approximately 80% of cases [1]. Histopathologically, AD is characterized by the extracellular accumulation of aggregated misfolded amyloid-β peptide (senile or amyloid plaques) and neurofibrillary tangles of hyperphosphorylated tau protein [2], in addition to astroglial changes that precede and accompany neuronal alterations [3, 4]. Clinically, AD is characterized by memory loss, language impairment, and behavioral changes, leading to functional and social disability [5]. In more than 95% of AD cases, the disease is sporadic, and the main risk factor is aging [6, 7].

Among the methods used to mimic the sporadic model of AD in rodents and primates is the intracerebroventricular

✉ Vanessa-Fernanda Da Silva
vanessafernanda171191@gmail.com;
s.vanessa1191@edu.pucrs.br

1 Programa de pós- graduação em Bioquímica, Universidade Federal do Rio Grande do Sul (UFRGS), Porto Alegre, Brazil

2 Programa de pós- graduação em Neurociências, Universidade Federal do Rio Grande do Sul (UFRGS), Porto Alegre, Brazil

3 Programa de pós-graduação em Biologia Celular e Molecular, Pontifícia Universidade Católica do Rio Grande do Sul (PUCRS), Porto Alegre, Brazil

administration of streptozotocin, a glucosamine-nitrosourea compound, which initially induces glucose hypometabolism in the central nervous system (pre-amyloid phase) and, within a few months, an increase and deposition of amyloid-β peptides (amyloid phase) [8, 9]. We have used this model to investigate astroglial alterations in both the pre-amyloid and amyloid phases [3, 10, 11].

Although the exact mechanism of action of STZ in the CNS is unknown, this drug is also used to accelerate the appearance of pathognomonic signs of AD (i.e., amyloid plaques) in rodent genetic models of the disease, where it induces the expression of human amyloid precursor protein, which will generate amyloid peptides [12]. Furthermore, cortical astrocyte cultures exposed to STZ have impaired clearance of beta-amyloid peptides and begin producing APP protein [13]. These data reinforce the importance of this model for the study of AD [14].

We hypothesize that STZ may induce cellular senescence, which is characterized by cell cycle arrest, without loss of activity or apoptosis. Cell cycle arrest usually occurs in the G1 phase [15] and is not only related to cell replication, but also to morphological, metabolic, epigenetic, inflammatory changes and the oxidative state of the cell [16]. Senescent astrocytes can be evaluated by changes in general markers such as p16, β-galactosidase, Lamin B1, and senescence-associated secretory phenotype (SASP) [17].

In the central nervous system (CNS), astrocytes are more strongly impacted than neurons by transcriptional changes induced by aging (see [18] for a review). Although behavioral and cognitive changes are more related to changes in the hippocampal and neocortical regions, the greatest susceptibility to astroglial aging is observed in regions such as the hypothalamus and cerebellum. For this reason, it seems reasonable to evaluate STZ-induced senescence in hypothalamic astrocytes.

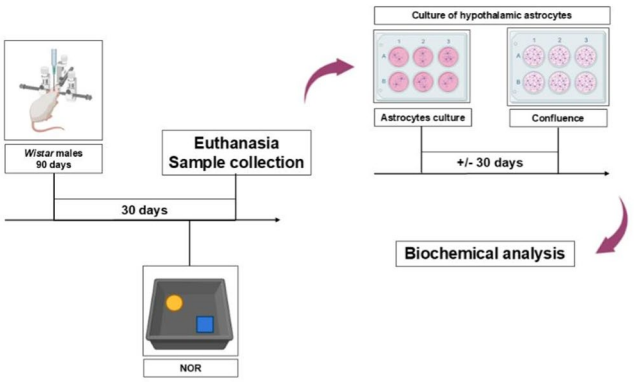


Fig. 1 Experimental design. Adult (90-day-old) male Wistar rats were subjected to the Alzheimer's type dementia model using intracerebroventricular (ICV) infusion of streptozotocin (3 mg/kg), or vehicle. Four weeks later, they were cognitively analyzed by the novel object recognition (NOR) test and subsequently euthanized. Hypothalamus were removed for astrocyte culture. Source: author's own work, BioRender

The STZ-induced Alzheimer's-type dementia model presents persistent astroglial changes lasting for months. It is possible that these changes would persist if astrocytes were isolated and cultured, expanding the possibilities for study and even therapeutic intervention. In the present study, we induced the dementia model and then isolated and cultured hypothalamic astrocytes, attempting to observe any persistent in vitro changes induced by STZ and confirm our hypothesis of senescence caused by this compound.

Methodology

Animals

Forty male 90-day-old Wistar rats (weight: 266 –383 g), obtained from the local breeding colony (CREAL-UFRGS), were transported and maintained in the Biochemistry department of the Universidade Federal do Rio Grande do Sul (UFRGS), Porto Alegre, Brazil, where the experiments were carried out. Animals were maintained under standard conditions, in a 12 h light/dark cycle, at a temperature of 24 ± 2 °C, and 50–60% relative humidity, with free access to water and food. All animal experiments were performed in accordance with the National Institutes of Health (NIH) Guide for the Care and Use of Laboratory Animals and were approved by the Animal Care and Use Committee of the Universidade Federal of Rio Grande do Sul (project number 41744).

Experimental Design

In this study, we used male Wistar rats that were subjected to a sAD model induced by STZ-ICV. At twenty-seven days after surgery, the animals underwent the recognition task. On day 30, the animals were briefly anesthetized with isoflurane and decapitated. The brains were dissected in a laminar flow hood, and primary hypothalamic astrocyte cultures were performed as described below. After culture confluence (approximately 30 days), the samples were lysed with buffers specific for each technique, and the samples were frozen in a -80 °C freezer until further analysis. The animals were randomly divided into two experimental groups: control and STZ (Fig. 1).

Novel Object Recognition (NOR) Task

The behavioral assessment employed was the NOR task, a straightforward memory evaluation that relies primarily on the rodent's natural exploration tendencies. The task consisted of three phases: habituation, training, and testing. All procedures were carried out during the animals' active

cycle, in an open-field apparatus measuring 50 cm x 50 cm. The animals were acclimated to the testing room for 1 h before the start of each phase of the experiment. On the first day, habituation was conducted, during which the animal was placed facing away from the center of the exploration apparatus for 10 min. On the second day, during the training phase, two identical objects (object A) were positioned diagonally in the peripheral area of the apparatus, allowing the animal to explore them for 5 min. After one hour, the short-term memory (STM) test was administered, in which one of the objects A was replaced with a novel object (object B), keeping the same location, with an exploration time of 5 min. On the third day, 24 h after training, the long-term memory (LTM) test was carried out, where object B was substituted with another new object (object C). The Recognition Index was determined using the following formula: (exploration time of the new object × 100) / (total exploration time of both objects) [3, 11].

Hypothalamic Astrocyte Culture

The hypothalami of two rats from the same group were removed in a laminar flow hood, and the preparation of the hypothalamic astrocyte cultures was based on previous protocols [19, 20]. The astrocytes were seeded (2–4 × 105 cells/cm^2) in culture dishes that were pre-coated with poly-L-lysine and cultured in DMEM/F12 (supplemented with 10% fetal bovine serum (FBS), 15 mM HEPES, 14.3 mM $NaHCO_3$, 2.5 mg/ml amphotericin B, and 0.05 mg/ml gentamicin) at 37 °C in an incubator with 5% CO_2. After 24 h, the culture medium was changed and, subsequently, replaced once every 3 days, until the cells reached confluence (approximately 30 days).

SASP Secretion by ELISA

To ensure the consistency of our results, the culture medium was replaced and, after 1 h, the conditioned medium was collected for Enzyme Linked Immunosorbent Assays (ELISA) analysis of the following secreted factors: BDNF, IL-6, S100B, and TNFα.

ELISAs were performed to evaluate the intra and extracellular levels of BDNF (Millipore Corporation, ref.: CYT306); HMGB1 (ELK Biotechnology, ref.: ELK1439); S100B (ELK Biotechnology, ref.: ELK2613); TNFα (Thermo Fischer Scientific, ref.: 88-7340). All procedures were carried out following the manufacturers' instructions. The results are expressed as percentages of the control group.

For GFAP levels, ELISA was performed with some modifications, as described by [21]. Briefly, samples were plated onto 96-well high-binding microplates and incubated overnight at 4 °C. Samples were previously diluted in PBS. A standard curve ranging from 0.1 to 10 ng of human GFAP was supplemented with bovine serum albumin (BSA) to give a final quantity of 100 ng/well (diluted in PBS). The plate was blocked with 5% BSA diluted in PBS for 2 h at room temperature. After blocking, anti-GFAP antibody diluted 1:1000 (polyclonal-DAKO, Z0334) in 0.5% BSA/PBS was added and incubated for 1 h at 37 °C. The secondary peroxidase-conjugated anti-rabbit antibody, diluted 1:1000, was then added for 1 h at 37 °C. Subsequently 0.2 mL of peroxidase substrate (Sigma Fast OPD) were added and incubated for 30 min in the dark. The reaction was stopped by the addition of 50 uL 3 M HCl and the absorbance was read at 492 nm on a Thermo Scientific Varioskan Lux spectrophotometer. Three washes were performed with 0.05% Tween-20, diluted in PBS, between each step. The results are expressed as percentages of the control.

Western Blotting

To perform Western Blotting, astrocyte culture samples were previously homogenized in 4% SDS Stopping Solution (Stopping A) and boiled at a temperature of ≥ 95 °C for 5 min, to denature proteins. After this procedure, the samples were centrifuged at 10,000 X g for 10 min, and the supernatants were collected for the following steps. From the aliquot, 5 µL were used in duplicate for the total protein dosage, using Peterson's modified Lowry's method [3]. Glycerol Sample Dilution Solution (40%; Stopping B) was then added to the remaining volume of the sample, before vortexing and storage in a -20 °C freezer until further analysis. After the quantification of total proteins, equal amounts of each tissue sample (20–30 µg), were separated by SDS polyacrylamide gel electrophoresis. Separated proteins were transferred to a 0.45–0.2 µm nitrocellulose membrane. The transfer procedure was confirmed with Ponceau-S staining. Membranes were blocked with a solution of 2% BSA in TBST for 2 h at room temperature (RT). After blocking, membranes were incubated with the corresponding primary antibodies overnight at 4 °C, followed by the respective secondary antibodies conjugated to peroxidase for 2 h at RT (see Table 1). Following secondary antibody incubation, the membranes were stored in TBS for the reading procedure. Between each step, washes with TBST were performed. The nitrocellulose membranes were reused after hydrogen peroxide stripping for different primary antibodies. The chemiluminescence signal was detected using ECL Super Signal West Pico Plus (Thermo Fisher) in a Chemidoc MP (Bio-Rad Laboratories). The optical densities of the images obtained were calculated with the ImageLab software (Bio-Rad Laboratories), and results were normalized

Table 1 List of antibodies used

Antibody	% of gel	RRID number	Dilution	Incubation
Anti-GFAP	12	Sigma, G9269	1:1000	1 ON 4 °C
Anti-Glast	12	Abcam, 963,286	1:1000	1 ON 4 °C
Anti-GLT-1	12	Abcam, GR124542-1	1:1000	1 ON 4 °C
Anti-GS	12	Santa Cruz, sc-32,560	1:1000	1 ON 4 °C
Anti-Lamin B1	12	Elabscience, E-AB-20,076	1:1000	1 ON 4 °C
Anti-mouse-HRP	–	Invitrogen, 31,430	1:10000	2 h RT
Anti-p16	16	ELK, ES8349	1:1000	2 ON 4 °C
Anti-p21	16	Elabscience, E-AB-66,357	1:1000	2 ON 4 °C
Anti-p53	12	DAKO, M7001	1:1000	1 ON 4 °C
Anti-rabbit-HRP	–	Elabscience, E-AB-1058	1:10000	2 h RT
Anti-β-actin-HRP	–	Proteintech, HRP600008	1:30000	2 h RT

GFAP glial fibrillary acidic protein, *Glast* Glutamate/Aspartate Transporter, *GLT-1* Glutamate Transporter-1, *GS* glutamine sintetase, *HRP* horseradish peroxidase, *ON* overnight, *RT* room temperature, *RT* room temperature

Table 2 Genes analyzed by quantitative RT-PCR

mRNA target	Assay ID
β-actin	Rn00667869_m1
C/EBP homologous protein (CHOP)	Rn00492098_g1
CDKN1A/p21^{Cip1} (p21)	Rn00589996_m1
CDKN2A/p16^{INK4a} (p16)	Rn00580664_m1
Forkhead Box O-3a (FOXO3a)	Rn01441087_m1
NF-E2-related factor 2 (Nrf2)	Rn00582415_m1
Nuclear factor kappa B (NFκB)	Rn01399572_m1
Sorcin	Rn01529190_m1

using β-Actin density and presented as percentage of the control group.

RNA Extraction and Quantitative RT-PCR

Total RNA was isolated from astrocyte cultures using TRIzol Reagent, and the concentration and purity of the RNA were determined spectrophotometrically at a ratio of 260:280 nm using Biodrop. One µg of RNA was then submitted to cDNA synthesis using the High-Capacity cDNA Reverse Transcription Kit (Applied Biosystems/Thermo Fisher Scientific). Quantitative determination of the messenger RNA (mRNAs) targets was performed using the TaqMan real-time RT-PCR system, with inventory primers and probes purchased from Applied Biosystems (Thermo Fisher Scientific), as described in Table 2. Target mRNA levels were normalized to β-actin levels, and the results were analyzed employing the $2^{-\Delta\Delta Ct}$ method [11].

Immunofluorescence

Cell cultures were incubated with 4% paraformaldehyde for 20 min, permeabilized with 0.1% Triton X-100 in PBS for 5 min at room temperature, and then blocked with 5% BSA for 45 min. Once blocked, cells were incubated overnight with anti-p53 antibody (DAKO, ref: M7001) diluted 1:250 in PBS at 4 °C, followed by washes with PBS and incubation with a specific secondary antibody conjugated with Alexa Fluor® 555 (1:1000) for 1 h at room temperature. The primary antibody was omitted for all negative immunofluorescence control responses. No reactivity was observed when the primary antibody was excluded. Cell nuclei were stained with 0.2 mg/ml 4',6'-diamino-2-phenylindole (DAPI). Astrocytes were spotted and imaged with a Nikon-specific TE-FM Epi-Fluorescence accessory [22].

GSH Content Measurement

GSH content was determined as previously described [23]. Briefly, the astrocyte cultures were homogenized in a sodium phosphate buffer (0.1 M, pH 8.0) containing 5 mM EDTA, and protein was precipitated with 1.7% meta-phosphoric acid. Supernatant was assayed with o-phthaldialdehyde (1 mg/mL of methanol) at room temperature for 15 min. Fluorescence was measured using excitation and emission wavelengths of 350 and 420 nm, respectively. A calibration curve was performed with standard glutathione solutions (0–500 mM). The GSH concentrations are expressed as nmol/mg protein [24].

Protein Content

Total protein content was determined by the Peterson modification of the Lowry method, as previously described [25], using BSA as standard [24].

Statistical Analysis

The animals were randomly assigned to experimental groups using an online random number generator. Descriptive statistical analysis and assessment of data normality were first performed using the Shapiro–Wilk test. Considering that all data were parametric, the results are presented as means ± standard deviation (SD). For NOR analysis, the one sample T test was used to evaluate differences between the Recognition Index from a chance performance of 50%. For other data, differences between Control and STZ groups were statistically analyzed using Student's t test, and the

value of $p < 0.05$ was used as a criterion for statistical significance. All analyses were performed using GraphPad Prism 9 (GraphPad Software, Inc., La Jolla, CA, USA).

Results

Primary Cultures of Astrocytes from Rats with STZ-Induced Cognitive Impairment

To confirm the validity of the dementia model, we performed a NOR task on rats that had received STZ via ICV four weeks previously. Our results confirm the successful induction of the sAD model whereby, in contrast to the control group, the STZ group demonstrated no significant preference for the novel object when compared to the 50% chance level, both at 1 h and at 24 h. This lack of preference at both timepoints indicated short-term memory impairment (Supplementary Fig. 1A, control $p = 0.0017$, STZ $p = 0.1427$) and long-term memory impairment (Supplementary Fig. 1B, control $p = 0.0016$, STZ $p = 0.1059$), respectively.

Characterization of Cultured Astrocytes from STZ Rats

We initially assessed the purity of the astroglial cultures after confluence. Over 95% of the cells were positive for GFAP. No quantitative difference in GFAP was observed between the STZ animal cultures and control animal cultures, when evaluated both by Western blotting (Fig. 2B, $p = 0.3526$) and by ELISA (Fig. 2A, $p = 0.5282$).

To assess the activity of cultured astrocytes, we quantitated the glutamine synthetase (GS) enzyme, which is responsible for glutamine synthesis, as well as the glutathione (GSH, an antioxidant) produced. We found a decrease in the amount of GSH in cultures from STZ animals (Fig. 2C, $p = 0.0112$), as well as a reduction in the amount of GS in hypothalamic cultures from STZ animals (Fig. 2D, $p = 0.0177$). Considering these changes in GS and GSH, we also evaluated the glutamate transporters, GLAST and GLT-1 (Supplementary Fig. 2A, $p = 0.1200$ and Supplementary Fig. 2B, $p = 0.7815$, respectively), and observed no changes in the quantities of these transporters.

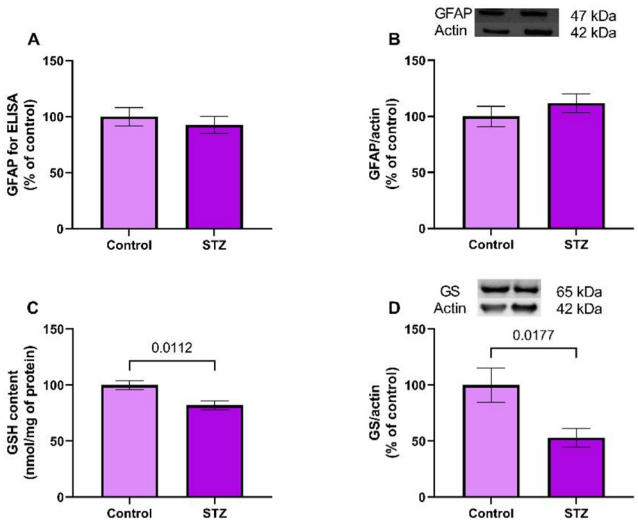


Fig. 2 Astroglial markers in primary cultures of animals treated with STZ. GFAP content measured by ELISA in **A** and Western blotting in **B** of hypothalamic astrocytes from STZ-ICV rats; Content of reduced glutathione (GSH), measured by OPT assay in **C**; and glutamine synthetase (GS) content measured by Western blotting in **D**. All data are represented as percentages relative to the control group ($n = 6$). Groups were compared using Student's t-test, and a p-value < 0.05 was considered statistically significant

Cultured Astrocytes from STZ Animals Exhibit a more Senescent Profile

Cellular senescence leads to an increase and accumulation of specific cell cycle arrest markers, as well as nuclear alterations. As such, we evaluated the gene expression and/or protein content of p53, p21, p16 and Lamin B1. The p53 protein content was increased in astrocyte cultures from STZ-treated animals (Fig. 3A, $p = 0.0084$ and Fig. 3B, $p = 0.0127$), as shown by western blotting and cellular immunofluorescence, respectively. Protein p21 exhibited an increase in content and gene expression in STZ animal cultures (Fig. 3C, $p = 0.0458$ and Fig. 3D, $p = 0.0022$). In contrast, p16 protein content was not altered in STZ animal cultures compared to control controls; however, a significant increase in gene expression was observed (Fig. 3E, $p = 0.5013$ and Fig. 3F, $p = 0.0080$). Furthermore, we also found no difference in Lamin B1 protein content in the astrocyte cultures from STZ animals (Fig. 3G, $p = 0.3601$). The image in Fig. 3H is representative of the immunofluorescence assays of astrocytic cultures for p53 (quantified in Fig. 3B).

S100B Secretion is Increased in Senescent Astrocytes

In addition to general senescence markers, we investigated the expression of some of the astrocytic Senescence-Associated Secretory Phenotype (SASP) proteins. The intracellular content of S100B, a specific astroglial protein, was not increased in cultures from animals treated with STZ (Fig. 4A, $p = 0.9665$), however a significant increase in basal secretion was observed at 1 h (Fig. 4B, $p = 0.0020$). Similarly, the intracellular content of High Mobility Group Box 1 (HGMB1) protein, considered a ubiquitous alarmin, was not increased in astrocytic cultures from animals treated with STZ (Fig. 4C, $p = 0.8740$), however, its basal secretion

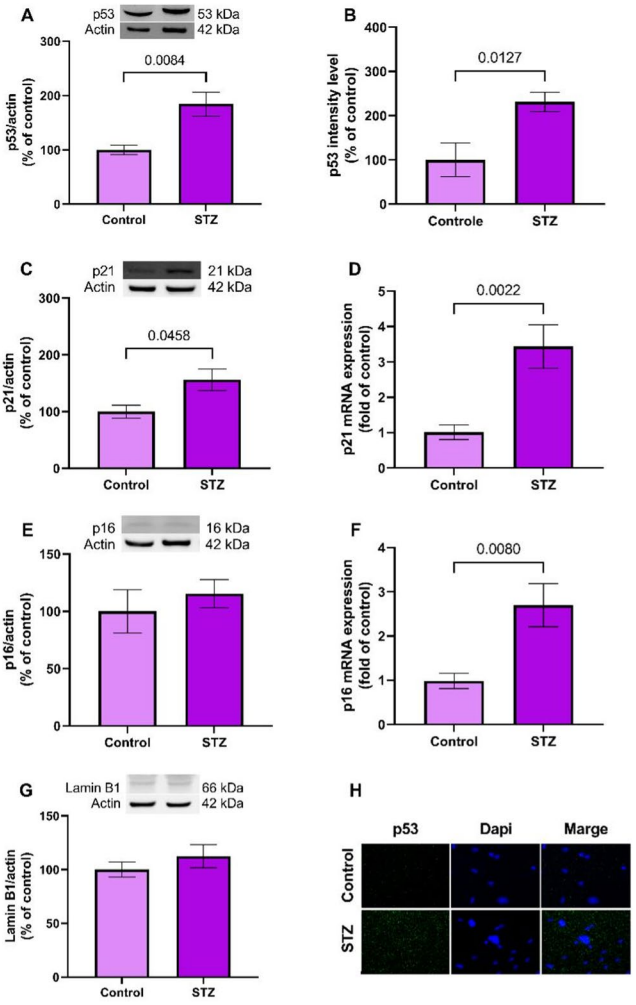


Fig. 3 Senescence markers in hypothalamic astrocyte cultures from STZ-ICV rats. Content of p53 measured by Western blotting in **A** and by immunofluorescence in **B** of control and STZ astrocytic cultures; content of p21, measured by Western blotting in **C**, and gene expression, measured by RT-qPCR in **D**; content of p16, measured by Western blotting in **E**, and gene expression, measured by RT-qPCR in **F**; Lamin B1 content, measured by Western blotting in **G**; Panel **H**, representative images of immunofluorescence for p53, with DAPI and merged. Data are represented as percentages or fold relative to the control group ($n = 5–6$). Groups were compared using Student's t-test, and a p-value < 0.05 was considered statistically significant

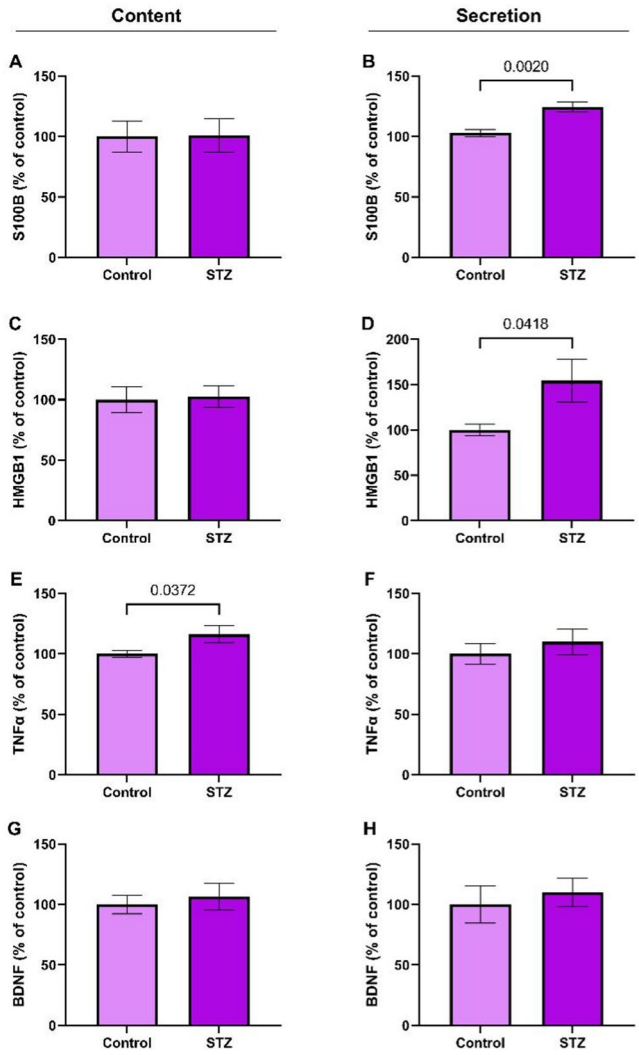


Fig. 4 Components of the secretome of cultured hypothalamic astrocytes obtained from ICV-STZ rats. Intracellular in **A** and extracellular in **B** S100B content of control and STZ astrocytic cultures; intracellular in **C** and extracellular in **D** HMGB1 content; intracellular **E** and extracellular **F** TNFα content; intracellular **G** and extracellular **H** BDNF content. All contents were determined by ELISA and data are represented as percentages relative to the control group ($n = 5–6$). Groups were compared using Student's t-test, and a p-value < 0.05 was considered statistically significant

was increased at 1 h (Fig. 4D, $p = 0.0418$). In contrast, the intracellular content of the TNFα cytokine was increased in astrocyte cultures from STZ animals (Fig. 4E, $p = 0.0372$), but basal secretion at 1 h was not altered (Fig. 4F, $p = 0.4813$). On the other hand, neither the intracellular content nor the basal secretion of the neurotrophin, BDNF, was altered in astrocyte cultures from STZ animals (Fig. 4G, $p = 0.6273$; Fig. 4H, $p = 0.6190$, respectively).

UPR Proteins are Elevated in Astrocyte Cultures from STZ Animals

To evaluate the unfolded protein response (UPR), commonly associated with aging and neurodegenerative disorders, we assessed the gene expression of sorcin and CHOP in astrocyte cultures from STZ animals. The expression of CHOP was increased 5-fold in astrocyte cultures from STZ animals (Fig. 5A, $p = 0.0222$), while sorcin expression increased by approximately 3-fold (Fig. 5B, $p = 0.0012$).

The FOXO3a Expression, as well as NFκB and Nrf2, is Increased in Senescent Astrocyte Cultures

The expression of FOXO3a is increased in senescent astrocyte cultures. To evaluate inflammaging, we investigated the gene expression of 3 transcription factors: NFκB, Nrf2, and FOXO3a. An approximately 3-fold increase in the expressions of NFκB (Fig. 6A, $p=0.0164$), Nrf2 (Fig. 6B, $p=0.0004$), and FOXO3a (Fig. 6C, $p=0.0164$) were observed in astrocyte cultures from STZ-treated animals.

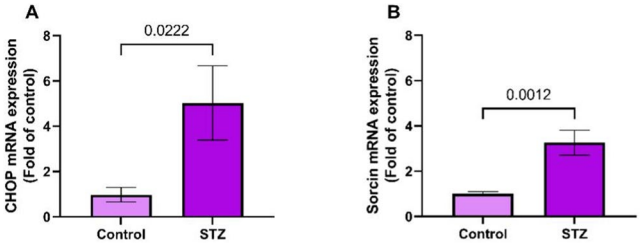


Fig. 5 Unfolded protein response markers in hypothalamic astrocyte cultures from STZ-ICV rats. Gene expression of CHOP in **A** and sorcin in **B** in control and STZ astrocytic cultures. Data are represented as fold relative to the control group ($n=5–6$). Groups were compared using Student's t-test, and a p-value <0.05 was considered statistically significant

Discussion

As the world's population ages, the prevalence of Alzheimer's disease (AD) is increasing [26]. Although AD shares several characteristics with normal brain aging [27], aging remains its greatest risk factor [28], highlighting the need to investigate new pharmacological strategies. In vivo administration of STZ has been widely used as a sporadic model of AD [3, 29–31], and more recently STZ has been used for in vitro models [13]. This study is the first to investigate changes in astrocyte cultures obtained from animals subjected in vivo to the Alzheimer's-type dementia model. The aim was to evaluate changes in senescence induced in vivo and maintained in vitro. Our findings indicate that the use of this model for studying the disease in vitro is promising and may facilitate the development of therapeutic intervention strategies.

Using primary hypothalamic astrocytes isolated four weeks after ICV-STZ administration, we investigated the relationship between cellular senescence and sAD, as well as a potential astrocyte-specific SASP. Cognitive impairment in the NOR test confirmed successful induction of the sAD model, consistent with previous reports [3, 8]. How aging remodels the CNS remains incompletely understood. The hypothalamus is particularly relevant because it regulates systemic metabolism and the HPA axis [18, 32]. Unlike other brain regions, it appears to exhibit limited astrocyte heterogeneity [33–37], suggesting that hypothalamic astrocytes may play a key role in aging and immunosenescence.

Astrocyte morphology assessment by simple phase contrast microscopy (data not shown) demonstrated no difference between astrocytic cultures of animals treated with STZ and control cultures. Similarly, no difference was observed in GFAP content in the STZ cultures, in contrast to the increase in GFAP observed in animals treated with STZ [3, 29]. Whether this reflects the model (in vivo vs. in vitro) or simply a regional response (hippocampus vs. hypothalamus) is not known at this time. However, both the GSH content, produced mainly by astrocytes [38, 39], and GS protein expression, which is specific to astrocytes in the brain tissue, were lower in hypothalamic astroglial cultures from animals treated with STZ, consistent with observations in the hippocampus of animals subjected to STZ dementia models [10, 40, 41].

Considering specific markers of senescence, we evaluated p53, known as the guardian of the genome [42, 43]. This protein's activity is strongly regulated by phosphorylation, which modulates its translocation to the nucleus [44–46]. We found an increase in p53 protein content in STZ animal astrocyte cultures, but we lack information about the phosphorylation or location of this protein. When we evaluated p21 in cultures from STZ animals, we also observed a substantial increase in both protein content and

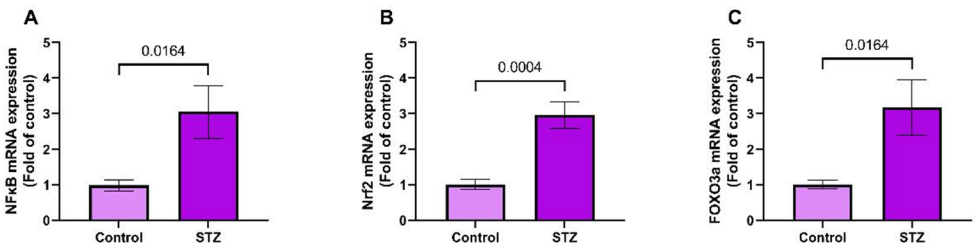


Fig. 6 Transcription factors associated with glial reactivity in hypothalamic astrocytes from STZ-ICV rats. Gene expression of NFκB in **A**, Nrf2 in **B**, and FOXO3a in **C** in control and STZ astrocytic cultures. All measurements were determined by RT-qPCR and data are represented as fold relative to the control group ($n=5–6$). Groups were compared using Student's t-test, and a p-value <0.05 was considered statistically significant

gene expression. Moreover, we observed an increase only in the expression of the p16 gene and not in its protein content, possibly because we are observing an early stage of senescence, occurring in STZ animals in the pre-amyloid phase of AD [3, 8].

When cellular senescence sets in, significant nuclear changes occur, including alterations in nuclear size and shape, as well as the formation of micronuclei [47], senescence-associated heterochromatin foci [48], and a decrease in Lamin B1 protein [49]. We herein evaluated the Lamin B1 protein content and observed no significant changes in astrocytes cultured from STZ-treated rats. Notably, a decrease in Lamin B1 is generally associated with an increase in the p16 tumor suppressor [49, 50]. In our study, p16 protein content also remained unchanged in the STZ-animal cultures, consistent with our findings for p53, p21, and sorcin, and suggestive of early changes in cellular senescence.

Senescent cells exhibit a cell-specific SASP [51]. We observed an increase in the extracellular medium content of S100B and HMGB1, with no change in intracellular content, suggesting that these proteins are secreted and may be part of the astrocytic SASP induced by STZ. Similarly to heat shock protein 70 (HSP-70), HMGB1 is a ubiquitous alarmin, while S100B is specific and secreted by astrocytes, working as an alarmin or cytokine [52–54]. We also evaluated the intracellular and extracellular levels of BDNF and TNFα, and observed no changes in BDNF, while TNFα was increased only in the cells. In addition to the classical senescence markers observed, the increase in extracellular S100B in astrocytes from rats exposed to STZ suggest that it is a component of the astrocytic SASP.

Metabolic shifts are directly linked to cellular senescence and, consequently, increases in ROS and RNS [55, 56], which can lead to endoplasmic reticulum (ER) stress [57]. Our group confirmed that the ICV-STZ model of dementia induces alterations in the UPR system in the hippocampus of animals, both at 4 and 16 weeks after model induction [11]. The UPR system plays a role in a complex and not yet understood sequence of events that are triggered by ER stress [58]. Accordingly, increased expressions of the proteins, C/EBP homologous protein (CHOP), which triggers apoptosis, and sorcin, a calcium-binding protein that neutralizes reticular calcium efflux [59, 60] were observed in astrocytes cultured from STZ animals, inferring the presence of ER stress. Interestingly, proteomic analysis of the cerebral cortex from AD patients demonstrated that sorcin is overexpressed, when compared to control individuals, especially in glial cells [61–63]. The ER is the main reservoir of cellular calcium, and ER stress not only increases intracellular calcium levels, but also impairs communication between the ER and mitochondria [57]. The changes in UPR observed indicate the presence of oxidative stress in our cell cultures, suggesting depletion of antioxidant molecules, which is consistent with our findings of decreased GSH. Note that although sorcin has the potential to reduce CHOP expression, in this STZ-induced UPR model, we observed an increase in the gene expression of both proteins [60].

Other notable characteristics of AD include neuroinflammation [2] and an increased redox state [64], which are also observed in the ICV-STZ model [9, 30, 40, 65, 66]. In astrocyte cultures from STZ animals, we observed an increase in the transcription factors, NF-κB and Nrf2, which are responsible for regulating these pathways, respectively. The increase in NF-κB is consistent with our finding of increased intracellular TNFα. Previous studies have demonstrated changes in both NF-κB [67] and Nrf2 [68] in the hippocampus of animals subjected to the same AD model. Interestingly, the FOXO3a transcription factor, whose expression was increased in the STZ-animal derived astrocyte cultures, directly and indirectly modulates the expression of both genes [69–72] and, in astrocytes, regulates the expression of proteins such as aquaporin-4 and GS [73, 74]. Moreover FOXO3a directly regulates the insulin pathway that modulates cell growth and proliferation [72]. Interestingly, the STZ-induced AD model displays glucose hypometabolism and insulin resistance in the CNS [3, 41].

It is important to acknowledge the limitations of this work. Although the changes in the STZ-ICV model are more frequently investigated in the hippocampus (due to its critical role in cognition), our cultures were performed from the hypothalamus tissue because it is highly susceptible to senescence, making it difficult to compare in vivo and in vitro results directly. Nevertheless, despite this limitation, our work provides important findings that improve our understanding of the role of cellular senescence in the STZ-induced AD model, since our cultures presented a persistent senescent phenotype, and aging remains the main risk factor for the development of this disease.

Conclusions

Our data demonstrate that hypothalamic astrocytes cultured from the ICV-STZ rat model of dementia of the Alzheimer's type exhibit increased senescence markers, such as p53, p21, and p16, as well as increased markers of oxidative stress and neuroinflammation, such as GSH, Nrf2, NFκB, and TNFα. See a summary of the results in Fig. 7. The increased S100B secretion in these cultures suggests that this protein can be incorporated as a component of the astrocytic SASP. Together, these data show that the cultured astrocytes from these animals preserve these alterations, allowing for a

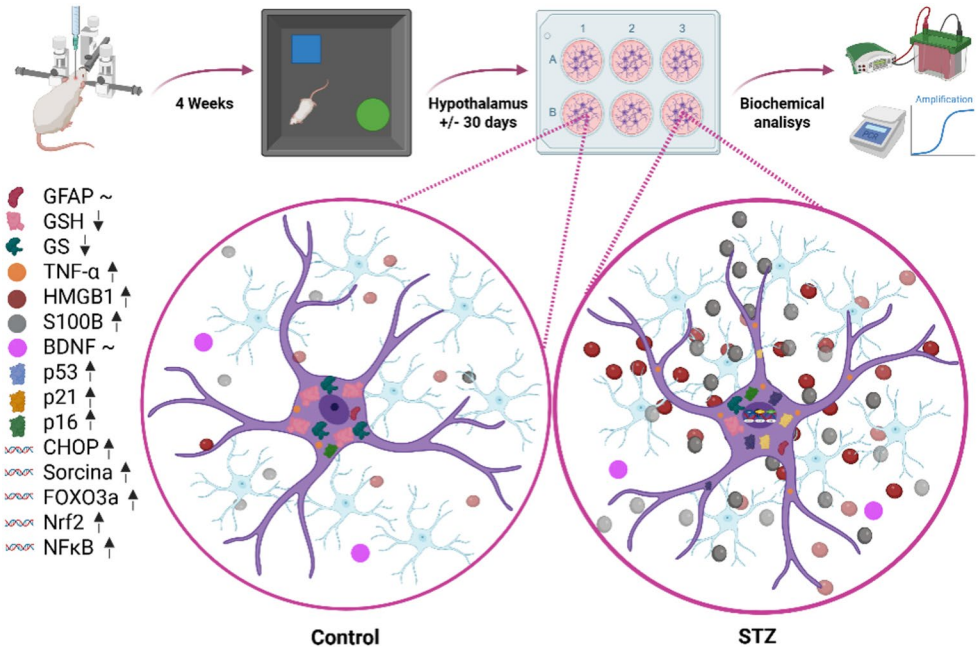


Fig. 7 Astroglial parameters in primary cultures of animals treated with STZ. Parameters analyzed are on the left and changes are represented by unchanged (~), increased (↑), or reduced (↓). Source: author's own work, BioRender

broader understanding of the model and the disease in vitro, for which age is the major risk factor.

Supplementary Information The online version contains supplementary material available at https://doi.org/10.1007/s11064-026-04884-7.

Acknowledgements We would like to thank everyone involved, directly and indirectly, as well as the funding agencies Conselho Nacional de Desenvolvimento Científico e Tecnológico (CNPq), Coordenação de Aperfeiçoamento de Pessoal de Nível Superior (CAPES) and Fundação de Amparo à Pesquisa do Estado do Rio Grande do Sul (FAPERGS), who provided support for this research.

Author Contributions VFS: Conceptualization, Investigation, Visualization, Writing and Original Draft, Writing and Review & Editing; DSC: Investigation, Writing and Review; VGD: Investigation, Writing and Review & editing; TMS: Investigation, Writing and Review; ACRS: Investigation, Writing and Review; BCRB: Investigation, Writing and Review; LFS: Investigation, Writing and Review; NS: Investigation, Writing and Review; FBW: Investigation, Writing and Review; IS: Investigation, Writing and Review; RAM: Investigation, Writing and Review; DNM: Investigation, Writing and Review; CAN: Writing and Review & Editing; LDB: Conceptualization, Funding Acquisition, Writing and Review & Editing; AQS: Conceptualization, Funding Acquisition, Writing and Review & Editing; CAG: Conceptualization, Funding Acquisition, Project Administration, Resources, Visualization, Writing and Original Draft, Writing and Review & Editing.

Funding The Article Processing Charge (APC) for the publication of this research was funded by the Coordenação de Aperfeiçoamento de Pessoal de Nível Superior - Brasil (CAPES) (ROR identifier: 00x0ma614). This work was supported by Conselho Nacional de Desenvolvimento Científico e Tecnológico (CNPq), Coordenação de Aperfeiçoamento de Pessoal de Nível Superior (CAPES) and Fundação de Amparo à Pesquisa do Estado do Rio Grande do Sul (FAPERGS).

Data Availability The data used to support the conclusions of this study are available from the corresponding author upon request.

Declarations

Competing interests The authors declare no competing interests.

Ethical Approval All animal experiments were performed in accordance with the National Institutes of Health (NIH) Guide for the Care and Use of Laboratory Animals and were approved by the Animal Care and Use Committee of the Universidade Federal of Rio Grande do Sul (project number 41744).

Open Access This article is licensed under a Creative Commons Attribution 4.0 International License, which permits use, sharing, adaptation, distribution and reproduction in any medium or format, as long as you give appropriate credit to the original author(s) and the source, provide a link to the Creative Commons licence, and indicate if changes were made. The images or other third party material in this article are included in the article's Creative Commons licence, unless indicated otherwise in a credit line to the material. If material is not included in the article's Creative Commons licence and your intended use is not permitted by statutory regulation or exceeds the permitted use, you will need to obtain permission directly from the copyright holder. To view a copy of this licence, visit http://creativecommons.org/licenses/by/4.0/.

References

1. Zou Y, Li L, Guan L et al (2023) Research trends and hotspots of glial fibrillary acidic protein within the area of Alzheimer's disease: a bibliometric analysis. Front Aging Neurosci 15. https://doi.org/10.3389/fnagi.2023.1196272
2. Heneka MT, Van Der Flier WM, Jessen F et al (2025) Neuroinflammation in Alzheimer disease. Nat Rev Immunol 25:321–352. https://doi.org/10.1038/s41577-024-01104-7
3. Gayger-Dias V, Menezes L, Da Silva V-F et al (2024) Changes in astroglial water flow in the pre-amyloid phase of the STZ model of AD Dementia. Neurochem Res 49:1851–1862. https://doi.org/10.1007/s11064-024-04144-6

4. Leclerc B, Abulrob A (2013) Perspectives in molecular imaging using staging biomarkers and immunotherapies in Alzheimer's disease. Sci World J 2013:589308. https://doi.org/10.1155/2013/589308
5. Soria Lopez JA, González HM, Léger GC (2019) Alzheimer's disease. Handbook of Clinical Neurology. Elsevier, pp 231–255
6. Zhang J, Zhang Y, Wang J et al (2024) Recent advances in Alzheimer's disease: mechanisms, clinical trials and new drug development strategies. Sig Transduct Target Ther 9:211. https://doi.org/10.1038/s41392-024-01911-3
7. Kelliny S, Lin L, Deng I et al (2021) A new approach to model sporadic Alzheimer's disease by intracerebroventricular streptozotocin injection in APP/PS1 mice. Mol Neurobiol 58:3692–3711. https://doi.org/10.1007/s12035-021-02338-5
8. Knezovic A, Osmanovic-Barilar J, Curlin M et al (2015) Staging of cognitive deficits and neuropathological and ultrastructural changes in streptozotocin-induced rat model of Alzheimer's disease. J Neural Transm 122:577–592. https://doi.org/10.1007/s00702-015-1394-4
9. Moreira AP, Vizuete AFK, Zin LEF et al (2022) The Methylglyoxal/RAGE/NOX-2 pathway is persistently activated in the hippocampus of rats with STZ-Induced sporadic Alzheimer's disease. Neurotox Res 40:395–409. https://doi.org/10.1007/s12640-022-00476-9
10. Brezolin ÉC, Gayger-Dias V, Da Silva V-F et al (2024) Astrocyte dysfunction alters GABAergic communication and ammonia metabolism in the streptozotocin-induced sporadic Alzheimer's disease model. J Alzheimer's Disease Rep 8:1381–1393. https://doi.org/10.1177/25424823241289036
11. Schultz B, Bobermin L, Menezes L et al (2025) Sex-Dependent Changes in the Gene Expression of UPR-Associated Calcium-Binding Proteins in the STZ–Induced Model of Alzheimer's Disease. Mol Neurobiol. https://doi.org/10.1007/s12035-025-05046-6
12. Plaschke K, Kopitz J, Siegelin M et al (2010) Insulin-resistant brain state after intracerebroventricular streptozotocin injection exacerbates Alzheimer-like changes in Tg2576 AβPP-overexpressing mice. JAD 19:691–704. https://doi.org/10.3233/JAD-2010-1270
13. Taday J, Fróes FT, Seady M et al (2024) In Vitro astroglial dysfunction induced by neurotoxins: Mimicking astrocytic metabolic alterations of Alzheimer's disease. Metabolites 14:151. https://doi.org/10.3390/metabo14030151
14. Chen Y, Liang Z, Blanchard J et al (2013) A non-transgenic mouse model (icv-STZ Mouse) of Alzheimer's disease: similarities to and differences from the transgenic model (3xTg-AD Mouse). Mol Neurobiol 47:711–725. https://doi.org/10.1007/s12035-012-8375-5
15. Kumari R, Jat P (2021) Mechanisms of cellular senescence: cell cycle arrest and senescence associated secretory phenotype. Front Cell Dev Biol 9:645593. https://doi.org/10.3389/fcell.2021.645593
16. Bhatia-Dey N, Kanherkar RR, Stair SE et al (2016) Cellular senescence as the causal nexus of aging. Front Genet 7. https://doi.org/10.3389/fgene.2016.00013
17. Pessoa B, Hayashide LDS, Dias G et al (2026) Senescent astrocytes: a new player in brain aging and cognitive decline. Brain Sci 16:76. https://doi.org/10.3390/brainsci16010076
18. Labarta-Bajo L, Allen NJ (2025) Astrocytes in aging. Neuron 113:109–126. https://doi.org/10.1016/j.neuron.2024.12.010
19. Santos CL, Bobermin LD, Quincozes-Santos A (2024) Aging changes the expression of adenosine receptors, insulin-like growth factor 1 (IGF1), and hypoxia-inducible factor 1α (HIF1α) in hypothalamic astrocyte cultures. Aging Brain 5:100104. https://doi.org/10.1016/j.nbas.2023.100104
20. Sovrani V, Bobermin LD, Sesterheim P et al (2023) Glioprotective effects of resveratrol in hypothalamic astrocyte cultures obtained from interferon receptor knockout (IFNα/βR–/–) mice. Vitro Cell-DevBiol-Animal. https://doi.org/10.1007/s11626-023-00777-z
21. Tramontina F, Leite MC, Cereser K et al (2007) Immunoassay for glial fibrillary acidic protein: antigen recognition is affected by its phosphorylation state. J Neurosci Methods 162:282–286. https://doi.org/10.1016/j.jneumeth.2007.01.001
22. Santos CL, Roppa PHA, Truccolo P et al (2018) Age-dependent neurochemical remodeling of hypothalamic astrocytes. Mol Neurobiol 55:5565–5579. https://doi.org/10.1007/s12035-017-0786-x
23. Browne RW, Armstrong D (1998) Reduced glutathione and glutathione disulfide. free radical and antioxidant Protocols. Humana, New Jersey, pp 347–352
24. Da Silva V-F (2024) Calorie restriction protects against acute systemic LPS-induced inflammation
25. Peterson GL (1977) A simplification of the protein assay method of Lowry et al. which is more generally applicable. Anal Biochem 83:346–356. https://doi.org/10.1016/0003-2697(77)90043-4
26. Gianfredi V, Nucci D, Pennisi F et al (2025) Aging, longevity, and healthy aging: the public health approach. Aging Clin Exp Res 37:125. https://doi.org/10.1007/s40520-025-03021-8
27. Ferrer I (2022) Alzheimer's disease is an inherent, natural part of human brain aging: an integrated perspective. Free Neuropathology 17 Seiten. https://doi.org/10.17879/FREENEUROPATHOLOGY-2022-3806
28. Hou Y, Dan X, Babbar M et al (2019) Ageing as a risk factor for neurodegenerative disease. Nat Rev Neurol 15:565–581. https://doi.org/10.1038/s41582-019-0244-7
29. Biasibetti R, Almeida Dos Santos JP, Rodrigues L et al (2017) Hippocampal changes in STZ-model of Alzheimer's disease are dependent on sex. Behav Brain Res 316:205–214. https://doi.org/10.1016/j.bbr.2016.08.057
30. Maheta P, Patel C, Parmar D et al (2025) Neuroprotective Effects of a 3-Amino Quinazoline Derivative via Keap1–Nrf2 Pathway Activation in an ICV-STZ-Induced Rat Model of Sporadic Alzheimer's Disease. ACS Chem Neurosci 16:3611–3622. https://doi.org/10.1021/acschemneuro.5c00540
31. Rodrigues L, Wartchow KM, Suardi LZ et al (2019) Streptozotocin causes acute responses on hippocampal S100B and BDNF proteins linked to glucose metabolism alterations. Neurochem Int 128:85–93. https://doi.org/10.1016/j.neuint.2019.04.013
32. Kim K, Choe HK (2019) Role of hypothalamus in aging and its underlying cellular mechanisms. Mech Ageing Dev 177:74–79. https://doi.org/10.1016/j.mad.2018.04.008
33. Kozareva V, Martin C, Osorno T et al (2021) A transcriptomic atlas of mouse cerebellar cortex comprehensively defines cell types. Nature 598:214–219. https://doi.org/10.1038/s41586-021-03220-z
34. Chai H, Diaz-Castro B, Shigetomi E et al (2017) Neural Circuit-Specialized Astrocytes: Transcriptomic, Proteomic, Morphological, and Functional Evidence. Neuron 95:531–549e9. https://doi.org/10.1016/j.neuron.2017.06.029
35. Sadick JS, O'Dea MR, Hasel P et al (2022) Astrocytes and oligodendrocytes undergo subtype-specific transcriptional changes in Alzheimer's disease. Neuron 110:1788–1805e10. https://doi.org/10.1016/j.neuron.2022.03.008
36. Hajdarovic KH, Yu D, Hassell L-A et al (2022) Single-cell analysis of the aging female mouse hypothalamus. Nat Aging 2:662–678. https://doi.org/10.1038/s43587-022-00246-4
37. Allen WE, Blosser TR, Sullivan ZA et al (2023) Molecular and spatial signatures of mouse brain aging at single-cell resolution. Cell 186:194–208e18. https://doi.org/10.1016/j.cell.2022.12.010

38. Chen Y, Qin C, Huang J et al (2020) The role of astrocytes in oxidative stress of central nervous system: A mixed blessing. Cell Prolif 53:e12781. https://doi.org/10.1111/cpr.12781
39. Dringen R, Arend C (2025) Glutathione Metabolism of the Brain—The Role of Astrocytes. J Neurochem 169:e70073. https://doi.org/10.1111/jnc.70073
40. Marschner RA, Ribeiro RT, Gayger-Dias V et al (2026) Increased type 3 deiodinase reduces hippocampal T3 signaling and is associated with cognitive impairment in a sporadic Alzheimer's disease animal model. Sci Rep. https://doi.org/10.1038/s41598-026-43232-1
41. Dos Santos JPA, Vizuete A, Hansen F et al (2017) Early and Persistent O-GlcNAc Protein Modification in the Streptozotocin Model of Alzheimer's Disease. JAD 61:237–249. https://doi.org/10.3233/JAD-170211
42. Park J, Zhuang J, Li J, Hwang PM (2016) p53 as guardian of the mitochondrial genome. FEBS Lett 590:924–934. https://doi.org/10.1002/1873-3468.12061
43. Zhang H, Xu J, Long Y et al (2024) Unraveling the Guardian: p53's Multifaceted Role in the DNA Damage Response and Tumor Treatment Strategies. IJMS 25:12928. https://doi.org/10.3390/ijms252312928
44. Castrogiovanni C, Waterschoot B, De Backer O, Dumont P (2018) Serine 392 phosphorylation modulates p53 mitochondrial translocation and transcription-independent apoptosis. Cell Death Differ 25:190–203. https://doi.org/10.1038/cdd.2017.143
45. Wang H, Guo M, Wei H, Chen Y (2023) Targeting p53 pathways: mechanisms, structures and advances in therapy. Sig Transduct Target Ther 8:92. https://doi.org/10.1038/s41392-023-01347-1
46. Meek DW, Anderson CW (2009) Posttranslational Modification of p53: Cooperative Integrators of Function. Cold Spring Harb Perspect Biol 1:a000950–a000950. https://doi.org/10.1101/cshperspect.a000950
47. Técher H, Gopaul D, Heuzé J et al (2024) MRE11 and TREX1 control senescence by coordinating replication stress and interferon signaling. Nat Commun 15:5423. https://doi.org/10.1038/s41467-024-49740-w
48. Ristori S, Bertoni G, Bigi A et al (2025) Human astrocytes from healthy individuals and Alzheimer's patients respond differently to Aβ1–42 oligomers, triggering distinct paths of reactivity and senescence. Mech Ageing Dev 228:112116. https://doi.org/10.1016/j.mad.2025.112116
49. Matias I, Diniz LP, Damico IV et al (2022) Loss of lamin-B1 and defective nuclear morphology are hallmarks of astrocyte senescence in vitro and in the aging human hippocampus. Aging Cell 21:e13521. https://doi.org/10.1111/acel.13521
50. Freund A, Laberge R-M, Demaria M, Campisi J (2012) Lamin B1 loss is a senescence-associated biomarker. MBoC 23:2066–2075. https://doi.org/10.1091/mbc.e11-10-0884
51. Limbad C, Oron TR, Alimirah F et al (2020) Astrocyte senescence promotes glutamate toxicity in cortical neurons. PLoS ONE 15:e0227887. https://doi.org/10.1371/journal.pone.0227887
52. Andersson U, Yang H, Harris H (2018) High-mobility group box 1 protein (HMGB1) operates as an alarmin outside as well as inside cells. Semin Immunol 38:40–48. https://doi.org/10.1016/j.smim.2018.02.011
53. Donato R, Sorci G, Riuzzi F et al (2009) S100B's double life: Intracellular regulator and extracellular signal. Biochimica et Biophysica Acta (BBA) -. Mol Cell Res 1793:1008–1022. https://doi.org/10.1016/j.bbamcr.2008.11.009
54. Gayger-Dias V, Vizuete AF, Rodrigues L et al (2023) How S100B crosses brain barriers and why it is considered a peripheral marker of brain injury. Exp Biol Med (Maywood) 15353702231214260. https://doi.org/10.1177/15353702231214260
55. Stojanovic B, Jovanovic I, Dimitrijevic Stojanovic M et al (2025) Oxidative Stress-Driven Cellular Senescence: Mechanistic Crosstalk and Therapeutic Horizons. Antioxidants 14:987. https://doi.org/10.3390/antiox14080987
56. Oliveira MCD, Schoffen JPF (2010) Oxidative stress action in cellular aging. Braz arch biol technol 53:1333–1342. https://doi.org/10.1590/S1516-89132010000600009
57. Ghemrawi R, Battaglia-Hsu S-F, Arnold C (2018) Endoplasmic Reticulum Stress in Metabolic Disorders. Cells 7:63. https://doi.org/10.3390/cells7060063
58. Bahar E, Kim H, Yoon H (2016) ER Stress-Mediated Signaling: Action Potential and Ca2 + as Key Players. IJMS 17:1558. https://doi.org/10.3390/ijms17091558
59. Gonçalves C-A, Sesterheim P, Wartchow KM et al (2022) Why antidiabetic drugs are potentially neuroprotective during the Sars-CoV-2 pandemic: The focus on astroglial UPR and calcium-binding proteins. Front Cell Neurosci 16:905218. https://doi.org/10.3389/fncel.2022.905218
60. Genovese I, Giamogante F, Barazzuol L et al (2020) Sorcin is an early marker of neurodegeneration, Ca2 + dysregulation and endoplasmic reticulum stress associated to neurodegenerative diseases. Cell Death Dis 11:861. https://doi.org/10.1038/s41419-020-03063-y
61. Tsuji T, Shiozaki A, Kohno R et al (2002) Proteomic Profiling and Neurodegeneration in Alzheimer's Disease
62. Umoh ME, Dammer EB, Dai J et al (2018) A proteomic network approach across the ALS - FTD disease spectrum resolves clinical phenotypes and genetic vulnerability in human brain. EMBO Mol Med 10:48–62. https://doi.org/10.15252/emmm.201708202
63. Andreev VP, Petyuk VA, Brewer HM et al (2012) Label-free quantitative LC–MS proteomics of Alzheimer's disease and normally aged human brains. J Proteome Res 11:3053–3067. https://doi.org/10.1021/pr3001546
64. Firdous SM, Chakrabortty S, Undale VR et al (2026) Interplay of oxidative stress and neuroinflammation in alzheimer's: insights into age-driven pathogenesis. https://doi.org/10.1007/s10787-026-02169-7. Inflammopharmacol
65. Dos Santos JPA, Vizuete AF, Gonçalves C-A (2020) Calcineurin-mediated hippocampal inflammatory alterations in streptozotocin-induced model of dementia. Mol Neurobiol 57:502–512. https://doi.org/10.1007/s12035-019-01718-2
66. Tiwari V, Mishra A, Singh S et al (2021) Protriptyline improves spatial memory and reduces oxidative damage by regulating NFκB-BDNF/CREB signaling axis in streptozotocin-induced rat model of Alzheimer's disease. Brain Res 1754:147261. https://doi.org/10.1016/j.brainres.2020.147261
67. Vizuete AFK, Moreira AP, Zin LEF et al (2025) Neuroprotective roles of metformin in a streptozotocin-induced dementia model in rats. Neurotox Res 43:48. https://doi.org/10.1007/s12640-025-00771-1
68. Firouzjaei Y, Hajizadeh Moghaddam A, Sohabatzadeh F et al (2026) Neuroprotective effects of plasma-activated N-acetylcysteine against streptozotocin-induced behavioral deficits in rats: Attenuation of oxidative stress and cholinergic dysfunction. Ecotoxicol Environ Saf 309:119619. https://doi.org/10.1016/j.ecoenv.2025.119619
69. Xu D, Qu X, Yang T et al (2024) The Foxo1-YAP-Notch1 axis reprograms STING-mediated innate immunity in NASH progression. Exp Mol Med 56:1843–1855. https://doi.org/10.1038/s12276-024-01280-5
70. Ferber EC, Peck B, Delpuech O et al (2012) FOXO3a regulates reactive oxygen metabolism by inhibiting mitochondrial gene expression. Cell Death Differ 19:968–979. https://doi.org/10.1038/cdd.2011.179
71. Jin H, Zhang L, He J et al (2022) Role of FOXO3a Transcription Factor in the Regulation of Liver Oxidative Injury. Antioxidants 11:2478. https://doi.org/10.3390/antiox11122478

72. Wang W, Zhu H, Jiang Q et al (2026) FOXO: a key target in regulating aging and age-related diseases. Biogerontology 27:38. https://doi.org/10.1007/s10522-025-10380-2
73. Saha P, Biswas SC (2015) Amyloid-β induced astrocytosis and astrocyte death: Implication of FoxO3a–Bim–caspase3 death signaling. Mol Cell Neurosci 68:203–211. https://doi.org/10.1016/j.mcn.2015.08.002
74. Kapoor S, Kim S-M, Farook JM et al (2013) Foxo3a Transcriptionally Upregulates AQP4 and Induces Cerebral Edema Following Traumatic Brain Injury. J Neurosci 33:17398–17403. https://doi.org/10.1523/JNEUROSCI.2756-13.2013

Publisher's Note Springer Nature remains neutral with regard to jurisdictional claims in published maps and institutional affiliations.